Journal of Sound and Vibration (2002) **251**(5), 905–918
doi:10.1006/jsvi.2001.4021, available online at http://www.idealibrary.com on IDEAL®

STRUCTURE-MODIFIED INFLUENCE ON THE INTERIOR SOUND FIELD AND ACOUSTIC SHAPE SENSITIVITY ANALYSIS

J. H. Wu† and H. L. Chen

Institute of Vibration and Noise Control, School of Mechanical Engineering, Xi'an Jiaotong University, Xi'an Shaanxi 710049, *People's Republic of China. E-mail*: *wwwjiuhui@263.net*

(*Received* 20 *November* 2000, *and in final form* 27 *June* 2001)

The covering-domain method is adopted to calculate first the interior sound field of a complex-shaped cavity stiffened with stringers, then the influence of an appended mass on the complex cavity wall is further analyzed based on the covering-domain method. Besides, the method is applied to analyze acoustic shape sensitivity of complex-shaped cavity. Combining a specific cavity, we calculate the corresponding acoustic shape sensitivity when every dimension of the cavity varies respectively. This will provide theoretical instruction for dynamic structural modification of the complex-shaped cavity.

1. INTRODUCTION

The interior sound field distribution of a cavity could be optimized or altered by dynamic structural modification in general. There are many optimizing measures in common use, such as appending stiffened stringer or a piece of mass, recomposing structural restrictions and altering wall-thickness or shape of the cavity. It is of important practical significance to analyze structure-modified influence on the interior sound field quantitatively.

For a complex-shaped closed shell, the substructure method [1] can be used to analyze the influence of stiffened stringer. But the method needs to obtain the mass, rigidity and damping matrixes of every subsystem, and to calculate eigenvalue of large matrix, which is time-consuming despite some mature arithmetic, such as sub-space method and Lanczaos method.

According to the principle of the covering-domain method [2, 3], it can be applied not only to calculate the interior sound field of complex-shaped cavity, but also to deal with the complex cavity with uneven wall-thickness. Therefore, in this paper, the covering-domain method is used to analyze the influence of a stiffened stringer on the internal sound field of the complex cavity, and further to study the influence of an appended mass.

In addition, acoustic shape sensitivity analysis is studied by adopting the covering-domain method in this paper.

Early in 1988, Aria *et al.* [4] analyzed acoustic shape sensitivity without considering vibroacoustic coupling. In 1991, Kane *et al.* [5] presented a shape design sensitivity analysis formulation by using the implicit differentiation of the discretized Helmholtz integral equation. In 1992, Smith and Bernhard [6] computed the sensitivity by differentiating the

†Present address: Institute of Acoustics, Nanjing University, Jiangsu Province, Nanjing 210093, People's Republic of China.

0022-460X/02/$35.00

discretized boundary integral equation. The derivative of the system matrix was approximated by adopting the finite difference concept. Although the finite difference method is straightforward and easily available for utilization, the method is not suitable for non-linear systems and has high computational cost owing to the reconstruction of the system matrix in order to adapt it for the perturbed shape.

In order to reduce the singularity of the sensitivity equation, the uniform potential field is brought into the solution process [7]. Because this potential-combined weakly singular sensitivity equation can increase the computational cost and requires singular integration to obtain an accurate solution, the sensitivity equation is further regularized and only the acoustic equation is used. The singularities of the integrands in the integral representation can be removed by adopting an integral identity utilizing the one-dimensional propagating wave component.

Therefore, we adopt the covering-domain method to analyze the acoustic shape sensitivity of the complex-shaped cavity, which has direct significance of optimizing its inside sound field by altering the structural shape.

2. THEORY OF THE COVERING-DOMAIN METHOD

Assume that the elastic objects A and B are, respectively, fixed in two separate co-ordinate systems. When the two co-ordinate systems are overlapped, it is concluded that B covers A if point $M \in A$, then $M \in B$.

In the general case, the boundary curved surface C of an arbitrary-shaped closed shell A can always be fitted by n pieces of spherical surfaces $C_1, C_2, \ldots, C_n$. To calculate the interior sound field of the closed shell A, a series of close spherical shells A_k ($k = 1, 2, \ldots, n$) can be used to cover A. The spherical shell A_k has only a piece of its boundary L_k to coincide with C_k and has the same thickness as the original spherical surface C_k. It is obvious that the common domain of all of A_k is the domain occupied by the closed shell.

Although it is difficult to calculate the interior sound field of a closed shell with complicated shape directly, it is easy to calculate the interior sound field of these spherical shells. So we can make use of the concept of covering-domain to change the problem of the interior sound field of a complicated shell into a simple problem of a series of closed spherical shells. Then the interior scattered sound field of the arbitrary-shaped closed shell can be expressed as follows:

$$P_S(\mathbf{r}) = \sum_{k=1}^{n} P_{SS}^{(k)}(\mathbf{r}), \tag{1}$$

where $P_{SS}^{(k)}(\mathbf{r})$ is the scattering sound field of the kth covering spherical shell at a point $\mathbf{r}$ inside the arbitrary-shaped closed shell.

According to references [2, 3], when there is a point sound source with unit strength at a point $\mathbf{r}_0(r_0, \theta_0, \varphi_0)$ inside a closed thin spherical shell, then the scattered sound pressure at an interior point $\mathbf{r}(r, \theta, \varphi)$ can be expressed as

$$P_{SS}(r, \theta, \varphi) = \sum_{n=0}^{\infty} \sum_{m=-n}^{n} C_n \, \mathrm{j}_n(kr) P_n^m(\cos\theta) \, \mathrm{e}^{\mathrm{i}m\varphi} \, \mathrm{e}^{-\mathrm{i}\omega t}, \tag{2}$$

where

$$C_n = \frac{b_{n1}}{a_{n2}} \frac{\mathrm{i}\omega}{4\pi c} (2n+1) \frac{(n-m)!}{(n+m)!} P_n^m(\cos\theta_0) \, \mathrm{e}^{-\mathrm{i}m\varphi_0} \, \mathrm{j}_n(kr_0),$$

$$a_{n2} = -a_{n1}\frac{\mathrm{j}_n'(kR)}{\rho c\omega} + b_n \mathrm{j}_n(kR), \qquad a_{n1} = a_n + b_n \frac{h_n^{(1)}(kR)}{h_n^{(1)'}(kR)}\omega\rho c,$$

$$b_{n1} = \frac{a_{n1}}{c}h_n^{(1)'}(kR) - b_n\omega\rho h_n^{(1)}(kR),$$

$$a_n = -\varepsilon n^3(n+1)^3 + \gamma_1 n^2(n+1)^2 - \gamma_2 n(n+1) + \gamma_3,$$

$$b_n = \frac{(1-\mu^2)R^2}{Eh}[-n(n+1) + (1-\mu) + k_t(kR)^2]$$

$$\times[1 - \varepsilon K_S(-n(n+1) + (1-\mu) + k_r(kR)^2],$$

$$\varepsilon = h^2/(12R^2), \qquad k_t = 1+\varepsilon, \qquad k_r = 1 + 3h^2/(20R^2), \qquad K_S = 2k_s/(1-\mu),$$

$$\gamma_1 = \varepsilon[3 - \mu - 2(1+\mu)k_s] + \varepsilon[k_t + k_r + k_t K_S](kR)^2,$$

$$\gamma_2 = 1 - \mu^2 - k_t(kR)^2 + 2\varepsilon[1 - \mu - (3 + 2\mu - \mu^2)k_s]$$

$$+ \varepsilon[(1-\mu)k_t + 2k_r - 2(1+\mu)k_r k_s - 4\mu k_t K_S](kR)^2$$

$$+ \varepsilon k_t[k_r + (k_t + k_r)K_S](kR)^2\omega^2,$$

$$\gamma_3 = [2(1-\mu^2) + (1+3\mu)k_t(kR)^2 - k_t^2(kR)^2\omega^2] - 4\varepsilon(1-\mu^2)k_s$$

$$- 2\varepsilon k_s[(1+3\mu)k_t + 2(1+\mu)k_r](kR)^2$$

$$+ \varepsilon k_t[2k_t k_s - (1+3\mu)k_r K_S](kR)^2\omega^2 + \varepsilon k_t^2 k_r K_S(kR)^2\omega^4,$$

where $k = \omega/c$ is the wave number, in which c is the sound velocity, $h_n^{(1)}(\cdot)$ is the first kind of the spherical Hankel function, $\mathrm{j}_n(\cdot)$ is the spherical Bessel function, and $P_n^m(\cdot)$ is the first kind of the associated Legendre function, h is the thickness of the spherical shell, R is the nominal radius of the closed spherical shell, E is the Young's modulus, μ is the Poisson ratio of the shell material, and k_s is an averaging coefficient of the shear, $\mathrm{i} = \sqrt{-1}$, ω is the circular frequency, and ρ is the media density.

Since expression (2) is deduced by a vibration equation satisfied by the closed thin spherical shell and the boundary conditions, the scattering from the shell to the outer infinite space is considered in calculating the interior scattering sound pressure by expression (2).

According to the acoustic reciprocity theory, to calculate the radiation sound pressure of an elastic object at a special point $\mathbf{r}_0$ due to the action of an external force, it is supposed that there is a point sound source q with unit strength at $\mathbf{r}_0$. If the scattered sound field $P_S(\mathbf{r}, \mathbf{r}_0)$ by the elastic object at a point $\mathbf{r}$ due to the action of the q is known, the radiation sound pressure of the elastic object at the point $\mathbf{r}_0$ excited by the external force can be calculated by the following equation:

$$P(\mathbf{r}_0) = -\frac{1}{\mathrm{i}4\pi\omega\rho}\iint_S \frac{\partial P_S(\mathbf{r}, \mathbf{r}_0)}{\partial \mathbf{n}}\cdot f(\mathbf{r})\,\mathrm{d}S, \tag{3}$$

where $f(\mathbf{r})$ is the distributive external force acting on the elastic object at $\mathbf{r}$, S is the elastic surface, $\mathbf{n}$ is the normal of the elastic surface which directs toward outside, $P(\mathbf{r}_0)$ is the radiation sound pressure at $\mathbf{r}_0$, and $P_S(\mathbf{r}, \mathbf{r}_0)$ is the scattered sound field by the elastic surface.

For a complex-shaped cavity, the interior scattering sound fields $P_S(\mathbf{r})$ can be obtained by equations (1) and (2), then the interior radiated sound field from the cavity excited by an external force can be obtained by equation (3).

Furthermore, in reference [2] the derivation of formula (2) makes it a condition that the spherical shell is thin-walled, i.e., $h \ll \lambda$, where λ is the wavelength of sound wave propagated in the shell material. Therefore, the valid frequency range in the covering-domain method is limited in $f \ll c_s/h$, where c_s is the sound velocity in the shell material.

3. STRUCTURE-MODIFIED INFLUENCE ON THE INTERIOR SOUND FIELD OF A COMPLEX-SHAPED CAVITY

3.1. INFLUENCE OF STIFFENED STRINGER ON THE INTERIOR SOUND FIELD OF A CAVITY

We have indicated that the covering-domain method can deal with the complex-shaped cavity that has equal or unequal wall-thickness in reference [2]. For uneven wall-thickness of the cavity, it can be fitted by the corresponding covering spherical shells with different thicknesses. Thus, when an arbitrary-shaped cavity wall is stiffened with stringers on the surface, we can consider the stiffened stringers as part of the thickness-increased wall.

In order to test the validity of the covering-domain method applied to the acoustic problem of a cavity stiffened with stringers, we fasten stiffened stringers on the surface of a rectangular chest. The chest is 1·2 m in length and 0·5 m in breadth and 0·8 m in height and all walls consist of steel plates of 2 mm in thickness. As shown in Figure 1, the orthogonal co-ordinates system is established and the positions of stiffened stringers are shown with grid in places 1 and 2 of the upper surface. In the first experiment, we fasten a piece of rectangular stringer on place 1, and in the second experiment, another piece of rectangular stringer is fastened on place 2. These rectangular stringers are all 0·5 m in length and 0·05 m in breadth and 0·007 m in height.

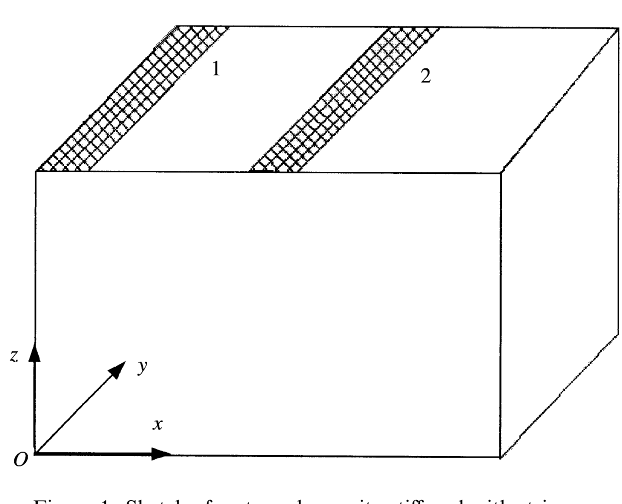

Figure 1. Sketch of rectangular cavity stiffened with stringers.

For such stiffened cavity, we measured the interior radiated sound field due to the action of single-point harmonic force. The experimental apparatus is the same as in reference [3]. In the two experiments, the excitation positions are located in the point (0·5, 0·33, 0·8), and the amplitudes of the driving forces are all regulated to 3 N.

When the covering-domain method is applied to do theoretical calculations for a rectangular chest, theoretically the more big the radii of the covering spherical shells are, the more fit to the walls of the chest is. But there exists a problem of numerical calculation here. Suppose the radius of the covering spherical shell is taken as r_p and the wave number is k_p, when $k_p r_p$ is very big, the series in expression (2) has low convergence and we have to calculate more terms of the series to obtain the accurate result. Because the factorial calculation with the higher order term is limited by computer capacity, the radius of the covering spherical shell cannot be taken infinite. In order to compare the effect of the different radius of the covering spherical shell to fit the wall of a rectangular chest, we have calculated the interior radiation sound pressures of the chest with the different radius of the covering spherical shell in reference [8] as shown in Figure 2. It can be seen from Figure 2 that when the radius of the covering spherical shell reaches 20 m, the results for 70 and 120 Hz are all steady and the radius of the covering spherical shell can take smaller value in the higher frequency. Therefore, for the rectangular chest stiffened with stringers, since every wall and the stringers are all flat, we select the radii of the covering spherical shells to be 20 m.

The comparisons between measured results and computed results of radiated sound pressure amplitudes at different interior points are listed in Tables 1–4.

From the above comparisons, we can find that the computed results are higher than the measured results. This may be due to two reasons. On the one hand, we have to use cohesion to adhere to the stiffened stringers on the chest surface in these experiments, which inevitably forms medium layer between them. Since the medium layer increases structural damping, which is not considered in the theoretical calculation, this will lead to the result that computed values are higher than the measured values. On the other hand, the wall opening in the experimental chest let out the internal sound pressure, which also is not considered in the theoretical calculations.

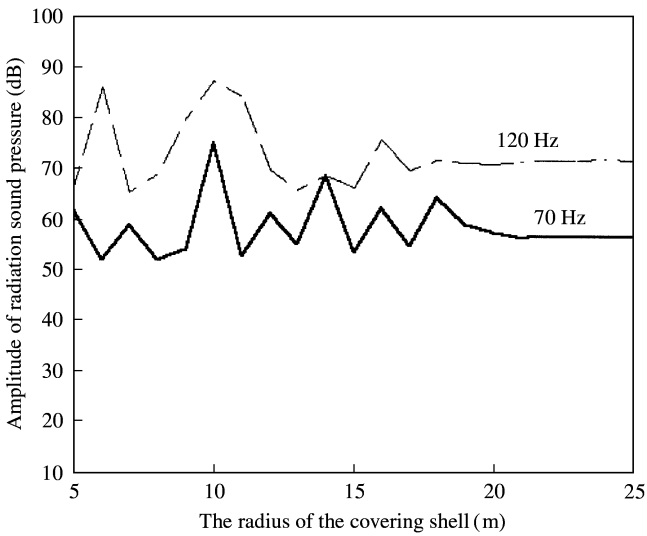

Figure 2. The effect of the different radius of the covering spherical shell to fit the wall of the rectangular chest.

TABLE 1

Comparisons for a stringer stiffened at 75 Hz driving frequency

Order	Co-ordinate positions x	y	z	Measured pressure (dB)	Calculated Pressure (dB)	Difference (dB)
1	0·9	0·25	0·5	81·9	85·1	− 3.2
2	0·9	0·25	0·3	82·5	85·5	− 3·0
3	0·8	0·25	0·5	83·3	85·6	− 2·3
4	0·8	0·25	0·3	84·3	86·3	− 2·0
5	0·7	0·25	0·5	83·5	86·4	− 2·9
6	0·7	0·25	0·3	82·6	83·3	− 3·2
7	0·6	0·25	0·5	83·1	84·7	− 1·6
8	0·6	0·25	0·3	84·7	83·3	1·4

TABLE 2

Comparisons for a stiffened stringer at 120 Hz driving frequency

Order	Co-ordinate positions x	y	z	Measured pressure (dB)	Calculated Pressure (dB)	Difference (dB)
1	0·9	0·25	0·5	84·7	87·7	− 3.0
2	0·9	0·25	0·3	87·4	90·1	− 2·7
3	0·8	0·25	0·5	84·5	87·5	− 3·0
4	0·8	0·25	0·3	86·7	90·3	− 3·6
5	0·7	0·25	0·5	85·9	88·6	− 2·7
6	0·7	0·25	0·3	87·2	90·4	− 3·2
7	0·6	0·25	0·5	85·1	88·6	− 3·5
8	0·6	0·25	0·3	88·2	90·5	− 2·3

TABLE 3

Comparisons for two stiffened stringers at 75 Hz driving frequency

Order	Co-ordinate positions x	y	z	Measured pressure (dB)	Calculated Pressure (dB)	Difference (dB)
1	0·9	0·25	0·5	77·5	81·3	− 3.8
2	0·9	0·25	0·3	75·3	78·0	− 2·7
3	0·8	0·25	0·5	79·5	81·8	− 2·3
4	0·8	0·25	0·3	76·8	78·9	− 2·1
5	0·7	0·25	0·5	82·7	84·9	− 2·2
6	0·7	0·25	0·3	77·2	80·0	− 2·8
7	0·6	0·25	0·5	84·3	85·6	− 1·3
8	0·6	0·25	0·3	77·7	80·6	− 2·9

Although there is a little discrepancy between the measured results and the computed results including random error in experiment, there is a good agreement between them. It is verified to be feasible that the covering-domain method can be adopted to deal with the acoustic problem of a stiffened complex cavity with stringers.

TABLE 4

Comparisons for two stiffened stringers at 120 Hz driving frequency

Order	Co-ordinate positions x	y	z	Measured pressure (dB)	Calculated Pressure (dB)	Difference (dB)
1	0·9	0·25	0·5	74·7	78·3	− 3.5
2	0·9	0·25	0·3	81·0	84·7	− 3·7
3	0·8	0·25	0·5	76·3	78·5	− 2·2
4	0·8	0·25	0·3	81·6	83·7	− 2·1
5	0·7	0·25	0·5	79·5	80·2	− 0·7
6	0·7	0·25	0·3	79·9	78·9	+ 1·0
7	0·6	0·25	0·5	81·4	81·3	+ 0·1
8	0·6	0·25	0·3	77·2	79·0	− 1·8

3.2. INFLUENCE OF AN APPENDED MASS ON THE INTERIOR SOUND FIELD OF CAVITY

Theoretically, the covering-domain method can also be adopted to deal with the acoustic problem that there is an appended mass on the surface of complex-shaped cavity. Whereas the interface of the appended mass is small, it is inconvenient to apply the method directly to deal with this acoustic problem. Here we present another method to solve this acoustic problem with an appended mass.

Considering a complex-shaped elastic closed cavity as shown in Figure 3, when a substance whose mass is m is appended on the cavity surface S_0, we need to study the influence of the appended mass m on the interior sound field of the closed cavity.

Without the appended mass, the interior scattered sound field $P_{S0}(\mathbf{r}, \mathbf{r}_0)$ of the complex-shaped cavity can be calculated by the covering-domain method. When the complex-shaped closed cavity is appended with mass we will first calculate its interior scattered sound field $P_{SS}(\mathbf{r}, \mathbf{r}_0)$.

Because the appended mass m is small, here we suppose that the appended mass does not bring deformation of the cavity surface S_1. And then the following equivalence theory comes into existence.

Supposing there is a point sound source q with unit strength at $\mathbf{r}_0(r_0, \theta_0, \varphi_0)$ inside the cavity, due to the action of the sound source q, the appended mass m vibrates harmonically, which can be considered equally as a harmonic force $F(\mathbf{r}_1)$ is acting on the cavity surface S_1. Therefore,

$$P_{SS}(\mathbf{r}, \mathbf{r}_0) = P_{S0}(\mathbf{r}, \mathbf{r}_0) + \left(-\frac{1}{4\pi \mathrm{i}\omega\rho}\right) \iint_{S_1} \frac{\partial P_{SS}(\mathbf{r}_1, \mathbf{r})}{\partial \mathbf{n}} \cdot F(\mathbf{r}_1)\, \mathrm{d}S, \tag{4}$$

where

$$F(\mathbf{r}_1) = -\, m\ddot{x}\bigg|_{S_0} = \frac{m}{\rho} \cdot \frac{\partial P_{SS}(\mathbf{r}_1, \mathbf{r})}{\partial \mathbf{n}}\bigg|_{S_0}, \tag{5}$$

where $\ddot{x}$ denotes vibration acceleration at S_0 of the cavity surface S_1, $\mathbf{n}$ is the outward normal vector of S_1.

Substituting equation (5) into equation (4), the result is

$$P_{SS}(\mathbf{r}, \mathbf{r}_0) = P_{S0}(\mathbf{r}, \mathbf{r}_0) - \frac{m}{4\pi \mathrm{i}\omega\rho^2} \iint_{S_0} \left[\frac{\partial P_{SS}(\mathbf{r}_1, \mathbf{r})}{\partial \mathbf{n}}\right]^2 \mathrm{d}S. \tag{6}$$

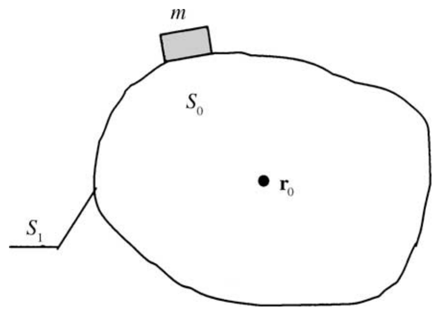

Figure 3. Appended mass on the surface of complex-shaped cavity.

Equation (6) belongs to the following non-linear Fredholm-type second integral equation:

$$\varphi(x) = f(x) + \lambda \int_a^b F(x, y, \varphi(y))\,\mathrm{d}y. \tag{7}$$

It can be proved [9], when the absolute value of parameter λ is properly small, the solution $\varphi(x)$ of Fredholm integral equation (7) exists, which can be constructed by using the following gradual approach method:

$$\varphi_0(x) = f(x), \qquad \varphi_n(x) = f(x) + \lambda \int_a^b F(x, y, \varphi_{n-1}(y))\,\mathrm{d}y \quad (n \geqslant 1). \tag{8a, 8b}$$

When $n \to \infty$, then $\varphi_n(x)$ tends towards the exact solution $\varphi(x)$.

When the mass m is small, the solution of integral equation (6) can be constructed by using the above gradual approach method. Considering the absolute value of $m/(4\pi \mathrm{i}\omega\rho^2)$ is quite small, we can take first order approximate value as the solution of integral equation (6). Thus,

$$P_{SS}(\mathbf{r}, \mathbf{r}_0) \approx P_{S0}(\mathbf{r}, \mathbf{r}_0) + \frac{m}{4\pi \mathrm{i}\omega\rho^2} \iint_{S_0} \left[\frac{\partial P_{S0}(\mathbf{r}_1, \mathbf{r})}{\partial \mathbf{n}}\right]^2 \mathrm{d}S. \tag{9}$$

The interior scattered sound field of the complex cavity with appended mass can be calculated by equation (9), so the internal radiated sound field of the closed cavity with the appended mass can be calculated by applying the reciprocity theory. Then the influence of the appended mass on the interior sound field of the complex-shaped closed cavity can be considered quantitatively.

According to the above equivalence theory, the influence of the appended mass on the interior sound field of the complex-shaped cavity corresponds to that of the external force driving on the cavity surface. In order to indicate the influence of the layout position of appended mass on the interior sound field of the cavity, we calculate theoretically the interior radiated sound field of the rectangular chest as shown in Figure 1 when the excitation position varies along the length direction of the chest. The calculated results are shown in Figure 4, and here the amplitude of the harmonic external force is 1 N, the calculated point in Figure 4(a) is located in (0·3, 0·12, 0·4) (the unit is meter), the calculated point in Figure 4(b) is located in (0·5, 0·32, 0·6). And the excitation position varies along the length direction of the chest, but y-co-ordinate and z-co-ordinate of the excitation position hold the line, they are 0·25 and 0·8 m respectively. In Figure 4, real line, dashed line, real line

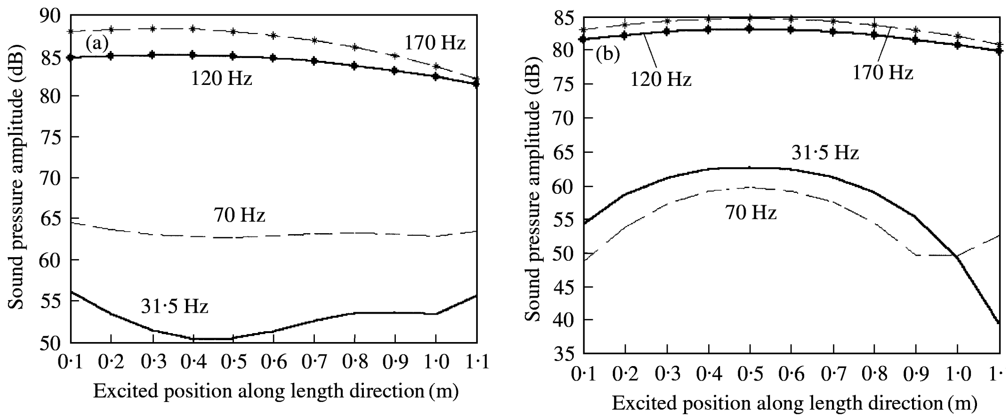

Figure 4. The interior sound pressure with different excitation frequency: (a) calculated point (0·3, 0·12, 0·4); (b) calculated point (0·5, 0·32, 0·6).

with star and dashed line with star denote the different calculated results when the driving frequencies are 31·5, 70, 120 and 170 Hz respectively.

From Figure 4 it can be found that the interior sound field is sensitive to the excitation position, especially in low-frequency band. For different response points, the driving frequency and frequency band to which the sound pressure is sensitive are different. This result is coincident to the practical testing from AUDI Corporation [10].

4. ACOUSTIC SHAPE SENSITIVITY ANALYSIS

Because the covering-domain method is based on the reciprocity theory, and the expression of the scattered sound field of the covering spherical shell is exact, the solution of the covering-domain method is theoretically analytical. In this section, we adopt the method to analyze the acoustic shape sensitivity of the interior sound field of complex-shaped cavity.

4.1. MATHEMATICAL DEFINITION OF SENSITIVITY

Sensitivity is a very broad concept, which has different specific meanings in different domains. But it can all be defined in mathematics as follows:

Supposing function $f(x)$ is differentiable, its one order sensitivity is defined as

$$s(f(x)) = \frac{\partial f(x)}{\partial x} \tag{10}$$

or

$$s(f(x)) = \frac{\Delta f(x)}{\Delta x}. \tag{11}$$

Equation (10) is the first order differential sensitivity, and equation (11) is the first order difference sensitivity. The following relative sensitivity is also in common use:

$$s(f(x)) = \lim_{\Delta x \to 0} \frac{\Delta f/f}{\Delta x/x} = \frac{x}{f}\frac{\partial f(x)}{\partial x} \quad f \neq 0. \tag{12}$$

Besides, there still are corresponding higher order sensitivities. The above sensitivities all reflect the influence degree of function $f(x)$ on the variation of parameter x.

4.2. THE RELATIVE SENSITIVITY OF INTERIOR SCATTERED SOUND FIELD OF SPHERICAL SHELL TO ITS PARAMETERS

When there is a point sound source with unit strength at a point $\mathbf{r}_0$ inside the spherical shell of wall-thickness h and radius R, we can apply equation (2) to further calculate the relative sensitivity of the scattered sound pressure at an internal point $\mathbf{r}$ of the spherical shell to its wall-thickness and radius.

The sensitivity of interior scattered sound field P_S of spherical shell to its radius R can be calculated by

$$\frac{\partial P_S}{\partial R} = \sum_{n=0}^{\infty} \sum_{m=-n}^{n} \frac{\partial C_n}{\partial R} \mathrm{j}_n(kr) P_n^m(\cos\theta)\, \mathrm{e}^{\mathrm{i}m\varphi}, \tag{13}$$

where

$$\frac{\partial C_n}{\partial R} = \frac{\mathrm{i}\omega}{4\pi c}(2n+1)\frac{(n-m)!}{(n+m)!} P_n^m(\cos\theta_0)\, \mathrm{e}^{-\mathrm{i}m\varphi}\, \mathrm{j}_n(kr_0) \frac{(\partial b_{n1}/\partial R)\, a_{n2} - b_{n1}\,(\partial a_{n2}/\partial R)}{a_{n2}^2},$$

b_{n1} and a_{n2} are the same as equation (2).

The sensitivity of interior scattered sound field P_S of spherical shell to its thickness h can be calculated by

$$\frac{\partial P_S}{\partial h} = \sum_{n=0}^{\infty} \sum_{m=-n}^{n} \frac{\partial C_n}{\partial h} \mathrm{j}_n(kr) P_n^m(\cos\theta)\, \mathrm{e}^{\mathrm{i}m\varphi}, \tag{14}$$

where

$$\frac{\partial C_n}{\partial h} = \frac{\mathrm{i}\omega}{4\pi c}(2n+1)\frac{(n-m)!}{(n+m)!} P_n^m(\cos\theta_0)\, \mathrm{e}^{-\mathrm{i}m\varphi_0}\, \mathrm{j}_n(kr_0) \frac{(\partial b_{n1}/\partial h) a_{n2} - b_{n1}\,(\partial a_{n2}/\partial h)}{a_{n2}^2},$$

b_{n1} and a_{n2} are also the same as equation (2).

The relative sensitivities of the scattered sound pressure at an internal point $\mathbf{r}$ of spherical shell to its wall-thickness and radius under different frequencies are shown in Figures 5 and 6 respectively. The basic parameters in the two figures are: the elastic modulus of the shell material $E = 2{\cdot}1 \times 10^{11}$ N/m^2, the Poisson ratio $\mu = 0{\cdot}3$, air media density $\rho_0 = 1{\cdot}29$ kg/m^3, sound velocity $c = 340$ m/s, and the point sound source is located at $\mathbf{r}_0 = (0{\cdot}08, \pi/3, \pi/6)$, the calculated point is located at $\mathbf{r} = (0{\cdot}12, 3\pi/4, 2\pi/3)$. In Figure 5 the spherical shell radius $R = 0{\cdot}18$ m, and in Figure 6 the spherical shell wall-thickness $h = 0{\cdot}002$ m.

In Figure 5, when the frequency is 70, 170 and 320 Hz in turn, the relative sensitivity of the internal scattered sound field of the spherical shell to its wall-thickness almost coincides, which indicates that the relative sensitivity is very insensitive to the frequency. When the spherical shell wall-thickness ranges between 0·0002 and 0·021 m, the relative sensitivity of the scattered sound field inside the spherical shell to its wall-thickness tends to show an exponential downtrend and it is very small, which shows that the interior scattered sound field is insensitive to variance in the wall-thickness.

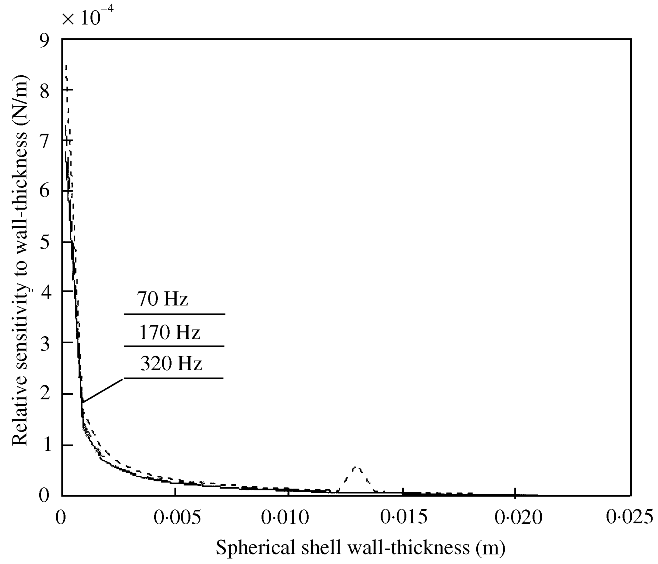

Figure 5. Relative sensitivity of interior scattered sound field of spherical shell to its wall-thickness.

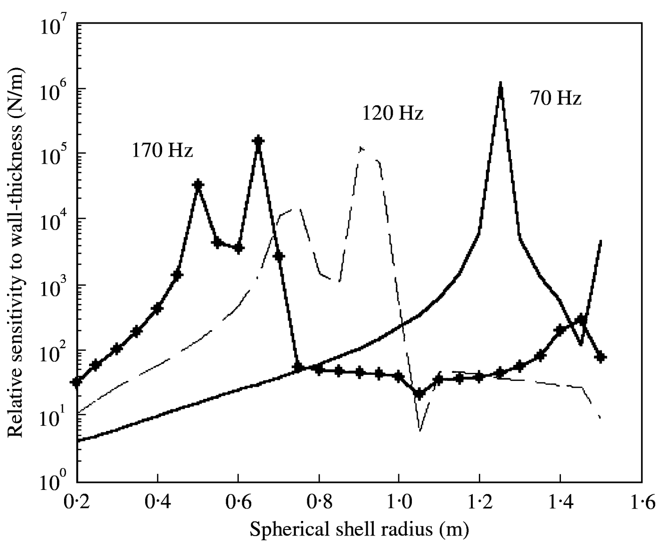

Figure 6. Relative sensitivity of interior scattered sound field of spherical shell to its radius.

From Figure 6 we can conclude that (1) the relative sensitivity of the scattered sound field inside the spherical shell to its radius is different with different frequency, (2) for different frequency, the radius corresponding to the extremum of the relative sensitivity is different, and (3) with increased frequency, the peak value of the relative sensitivity drifts towards smaller radius. This enables us to design specific structural shape with corresponding frequency.

4.3. THE ACOUSTIC SHAPE SENSITIVITY OF A RECTANGULAR CHEST

There is a rectangular chest with length $x = 1{\cdot}2$ m and breadth $y = 1{\cdot}0$ m and height $z = 0{\cdot}8$ m and wall-thickness $h = 0{\cdot}002$ m. When a harmonic force with amplitude A acts on the upper surface to the rectangular chest at a point $\mathbf{r}_j$, the sensitivity of the radiated sound pressure at an internal point $\mathbf{r}$ to the chest length x, breadth y and height z with two different frequencies 70 and 120 Hz are shown in Figures 7, 8 and 9 respectively. (a) and (b) in these figures show the internal sound pressure amplitude of the chest at different excitation positions respectively. Here the elastic modulus of the chest material is $E = 2{\cdot}1 \times 10^{11}$ N/m^2, the Poisson ratio $\mu = 0{\cdot}3$, air media density $\rho_0 = 1{\cdot}29$ kg/m^3, sound velocity $c_0 = 340$ m/s, $A = 3$ N and the calculated point is located at (0·55, 0·65, 0·67) in the three figures.

It can be found from these figures that when the calculated point position is fixed, the sensitivity of the sound pressure at the response point to the shape parameters of the chest is different with different driving frequency. In the same way, the sensitivity is also different with different excitation position. But at certain point inside the chest the sound pressure is

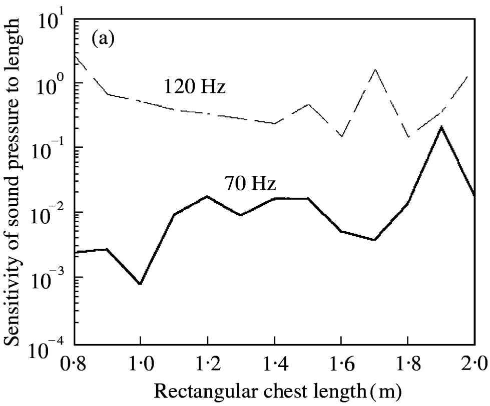

Figure 7. Sensitivity of interior sound pressure of rectangular chest to its length with different excitation frequency and driving position: (a) (0·4, 0·33, 0); (b) (0·65, 0·53, 0).

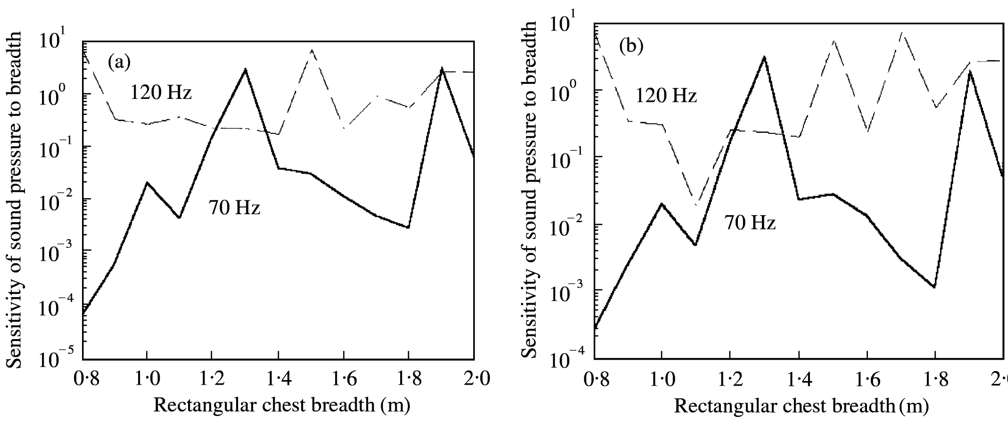

Figure 8. Sensitivity of interior sound pressure of rectangular chest to its breadth with different excitation frequency and driving position: (a) (0·4, 0·33, 0); (b) (0·65, 0·53, 0).

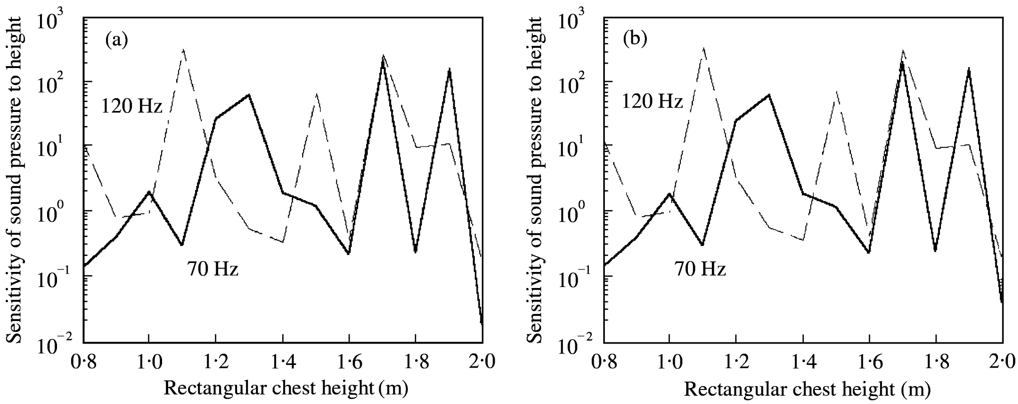

Figure 9. Sensitivity of interior sound pressure of rectangular chest to its height with different excitation frequency and driving position: (a) (0·4, 0·33, 0); (b) (0·65, 0·53, 0).

most sensitive to a certain direction. Therefore, even though for the same interesting response point, the acoustic shape sensitivity is different with different driving frequency and different excitation position. In order to optimize the internal sound field of a specific structure at certain optimizing position, the structural shape should be designed by the corresponding external excitation position and exciting frequency.

5. CONCLUSIONS

In this paper the covering-domain method is adopted to analyze first the influence of stiffened stringers on the internal sound field of a complex-shaped cavity, then the influence of an appended mass is further studied based on the covering-domain method. Besides, the method is applied to analyze acoustic shape sensitivity. Combining a specific cavity, we calculate the acoustic sensitivity due to shape variety of the cavity. This will provide a theoretical base for dynamic characteristic modification of the complex-shaped cavity.

ACKNOWLEDGMENTS

The authors wish to express their gratitude to the National Nature Science Foundation of China (No: 59875069) and the Doctorate Foundation of Xi'an Jiaotong University of China. The authors also wish to thank the anonymous reviewer for his (her) opinions.

REFERENCES

1. R. R. Craig Jr and M. C. Bampton 1968 *American Institute of Aeronautics and Astronautics Journal* **6**, 1313–1319. Coupling of substructures for dynamic analyses.
2. Wu Jiuhui, Chen Hualing and Hu Xuanli 2000 *Acta Acustica* **25**, 468–471. Method to calculate interior sound field of arbitrary-shaped closed thin shell.
3. J. H. Wu, H. L. Chen and W. B. An 2000 *Journal of Sound and Vibration* **237**, 793–803. A method to predict sound radiation from a plate-ended cylindrical shell excited by an external force.
4. A. Aria, I. Hagiwara and T. Nagabuchi 1988 *Proceedings of Symposium on Computation Methods in Structural Engineering and Related Fields*, New York, Vol. 12, 545–550. Sensitivity analysis of vehicle interior vibration and noise.

5. J. H. KANNE and S. MAO 1991 *Journal of the Acoustical Society of America* **90**, 561–573. A boundary element formulation for acoustic shape sensitivity analysis.
6. D. C. SMITH and R. J. BERNHARD 1992 *Transactions of the American Society of Mechanical Engineers*, *Journal of Vibration and Acoustic* **114**, 127–132. Computation of acoustic shape design sensitivity using a boundary element method.
7. B.-U. KOO, J.-G. IH, B.-C. LEE 1998 *Journal of the Acoustical Society of America* **104**, 2851–2860. Acoustic shape sensitivity analysis using the boundary integral equation.
8. J. H. WU 2001 *Ph.D. Thesis*, *Xi'an Jiaotong University of China*. The covering-domain method for vibroacoustic studies inside vehicle.
9. CHEN CHUANZHANG *et al*. 1987 *Integral Equation and its Application*, 12–22. Shanghai: Shanghai Science Technology Press.
10. X. HU 1997 *AUDI AG*. Tieffrequente Karosseriedrõhnen, Forschungsbericht.